PROCEEDINGS OF SCIENCE

Measurement of the ridge in pp and p+Pb collisions with the ATLAS detector at the LHC

Adam Trzupek on behalf of the ATLAS Collaboration*
Instiute of Nuclear Physics PAS
ul. Radzikowskiego 152
31-342 Kraków, Poland
E-mail: Adam.Trzupek@ifj.edu.pl

Recent measurements from the ATLAS experiment of the azimuthal anisotropy of charged hadron production in pp collisions at $\sqrt{s}$ = 2.76, 5.02 and 13 TeV and in p+Pb collisions at $\sqrt{s_{\rm NN}}$ = 5.02 TeV at the Large Hadron Collider (LHC) are presented. The measurements of the two-particle correlations (in $\Delta\eta, \Delta\phi$) using a template fitting procedure to remove correlations arising from hard-scattering processes are shown. The results on the per-trigger-particle yields, Y, as well as on $v_{\rm n}$ Fourier coefficients are presented as a function of the charged particle multiplicity, $N_{\rm ch}^{\rm rec}$, and transverse momentum, $p_{\rm T}$, for n = 2–4. Interestingly, v_2 values in pp collisions are found to be approximately constant as a function of multiplicity. The $p_{\rm T}$-dependence of $v_{\rm n}$ is similar to that measured in Pb+Pb collisions suggesting that in small systems features characteristic of the collective anisotropic flow are also present.

Fourth Annual Large Hadron Collider Physics
13-18 June 2016
Lund, Sweden

*Speaker.

PoS(LHCP2016)118

1. Introduction

The azimuthal anisotropy of hadron production is a key observable for understanding the properties of the hot and dense medium created in heavy-ion collisions at the LHC [1]. It is expected that the observed azimuthal anisotropy is sensitive to conditions at the very early stage of the evolution of the strongly coupled Quark-Gluon Plasma (QGP) and is related to the shape of the initial interaction region of colliding nuclei. The initial spatial asymmetry leads to asymmetric pressure gradients in the QGP, generating a significant azimuthal anisotropy in the final particle distribution dN/ϕ, which is usually described by means of a Fourier series with harmonics, $v_{\rm n} = \langle \cos n(\phi - \Phi_{\rm n})\rangle$, where ϕ is the particle azimuthal angle, $\Phi_{\rm n}$ represents the reaction plane angle and n is the flow harmonic order. The second harmonic, called elliptic flow (v_2), and higher-order flow harmonics characterise the "elliptical" shape of the initial interaction region and its higher modes, respectively. In the ATLAS experiment the azimuthal anisotropy was extensively explored in the 2.76 TeV Pb+Pb and 5.02 p+Pb data using a variety of methods [2–6], including the two-particle correlations (2PC) [7–9]. It is commonly accepted that in heavy ion collisions the azimuthal anisotropy of single particles is reflected in ridge-like structures in the 2PC function in relative $\Delta\phi, \Delta\eta$ of correlated particle pairs. Interestingly, the ridge-like structures in the 2PC function were not only observed in heavy-ion collisions but they were also found in pp [10,11] and p+Pb [9] collisions. As a consequence, a puzzling question arises whether the QGP is also present in small collision systems. In this report, the most recent ATLAS 2PC results for pp and p+Pb data are reviewed [11,12].

In ATLAS [13], flow phenomena are explored with charged particles reconstructed within the inner detector using the silicon pixel detector and the semiconductor micro-strip tracker (SCT), immersed in a 2 T axial magnetic field and covering a wide pseudorapidity range ($|\eta| <$2.5). The transverse momenta of reconstructed particles are limited by a minimum $p_{\rm T}$ of 0.3 GeV. The data samples of pp and p+Pb events used in the analysis were obtained by a combination of requirements at the level-1 (L1) and high level (HLT) trigger systems [8,12]. Especially, for the ridge study in pp and p+Pb collisions, a set of "high-multiplicity triggers" (HMT) was used by applying different thresholds imposed on the number of HLT-reconstructed tracks. These triggers enhance the number of collected events at high multiplicity during online data taking. As one can see in Fig. 1, multiplicity distributions for 5.02 and 13 TeV pp, and 5.02 TeV p+Pb collisions show significant enhancement in event statistics at high multiplicities.

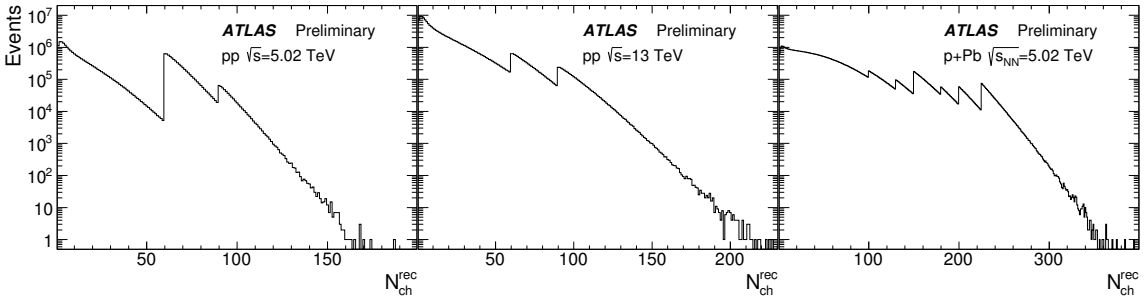

Figure 1: Distributions of the multiplicity, $N_{\rm ch}^{\rm rec}$, of reconstructed charged particles having $p_{\rm T} > 0.4$ GeV in the 5.02 TeV pp (left plot), 13 TeV pp (middle plot), and 5.02 TeV p+Pb (right plot) data used in this analysis. The discontinuities in the distributions correspond to different high-multiplicity trigger thresholds [12].

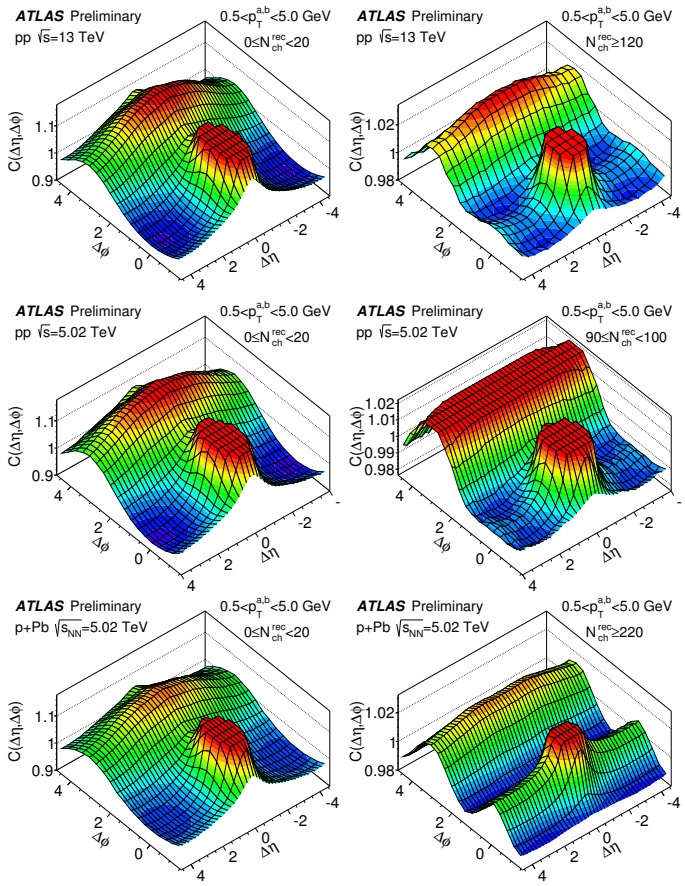

Figure 2: Two-particle correlation functions, $C(\Delta\eta,\Delta\phi)$, in 13 TeV pp collisions (top panels), 5.02 TeV pp collisions (middle panels) and in 5.02 TeV p+Pb collisions (bottom panels). The left panels correspond to a lower-multiplicity range of $0 \leq N_{\rm ch}^{\rm rec} < 20$. The right panels correspond to higher multiplicity ranges of $N_{\rm ch}^{\rm rec} \geq 120$ for 13 TeV pp, $90 \leq N_{\rm ch}^{\rm rec} < 100$ for the 5.02 TeV pp and $N_{\rm ch}^{\rm rec} \geq 220$ for the 5.02 TeV p+Pb. The plots are for charged particles having $0.5 < p_{\rm T}^{\rm a,b} < 5.0$ GeV. The distributions have been truncated to suppress the peak at $(\Delta\eta, \Delta\phi)$=(0,0) [12].

2. Two-particle correlation function

A commonly used tool to probe collective phenomena in heavy ion collisions is the two-particle correlation function in the relative pseudorapidity ($\Delta\eta$) and azimuthal angle ($\Delta\phi$) of correlated particle pairs. Recently, a two-particle correlation analysis was performed in ATLAS [11, 12] for pp collisions at $\sqrt{s} = 2.76$, 5.02 and 13 TeV and for p+Pb collisions at $\sqrt{s_{\rm NN}} = 5.02$ TeV using a novel template fitting procedure. Examples of two-dimentional 2PC correlation functions for charged particles in peripheral (low multiplicity) and central (large multiplicity) collisions are shown in Fig. 2. For peripheral collisions the correlation function shows a sharp peak centred at ($\Delta\phi$,$\Delta\eta$) = (0, 0) and a broad structure (in $\Delta\eta$) at $\Delta\phi \approx \pi$ (referred to as "recoil"), both predominantly originating from non-flow effects including particle pairs from the same jet, Bose-Einstein correlations, resonance decays or momentum conservation. In high-multiplicity collisions, in addition to the structure observed in low-multiplicity collisions, the correlation function reveals a broad

structure (in $\Delta\eta$) at $\Delta\phi \approx 0$, called also the "near-side ridge". The distribution at $\Delta\phi \approx \pi$ is also broadened relative to peripheral collisions, consistent with the presence of a long-range component (the "away-side ridge").

The strength of the long-range component is commonly quantified by the "per-trigger yield", $Y(\Delta\phi)$, which measures the average number of particle pairs correlated with a trigger particle. Figure 3 shows the $Y(\Delta\phi)$ distributions for $2 < |\Delta\eta| < 5$ in peripheral and central 13 TeV pp collisions (solid black points). To study the ridge, clearly seen in plots for central collisions at $\Delta\phi \approx 0$, the Y is fitted by a template function consisting of two components: a scaled per-trigger yield for low multiplicity interactions (open points in Fig. 3) and an azimuthal modulation term describing the "ridge" (dashed line):

$$Y^{\text{template}}(\Delta\phi) = FY^{\text{peripheral}}(\Delta\phi) + Y^{\text{ridge}}(\Delta\phi) \tag{2.1}$$

where

$$Y^{\text{ridge}}(\Delta\phi) = G(1 + \sum_{n=1}^{\infty} 2v_{\text{n,n}} cos(2\Delta\phi)). \tag{2.2}$$

The azimuthal modulation parameters $v_{\text{n,n}}$ and F are obtained from the fitting procedure while the parameter G is fixed by normalisation of the template function to the data. As it was reported in Ref. [11], the template fitting procedure only including the second-order harmonic $v_{2,2}$ can well describe the data in all multiplicity ranges, see Fig. 3. Additionally, it was demonstrated that apart from the elliptic modulation also a much smaller but significant triangular and quadrangular modulations are present with amplitudes $v_{\text{n,n}}$ about 30 times smaller than $v_{2,2}$. If $v_{\text{n,n}} \cos(n\Delta\phi)$

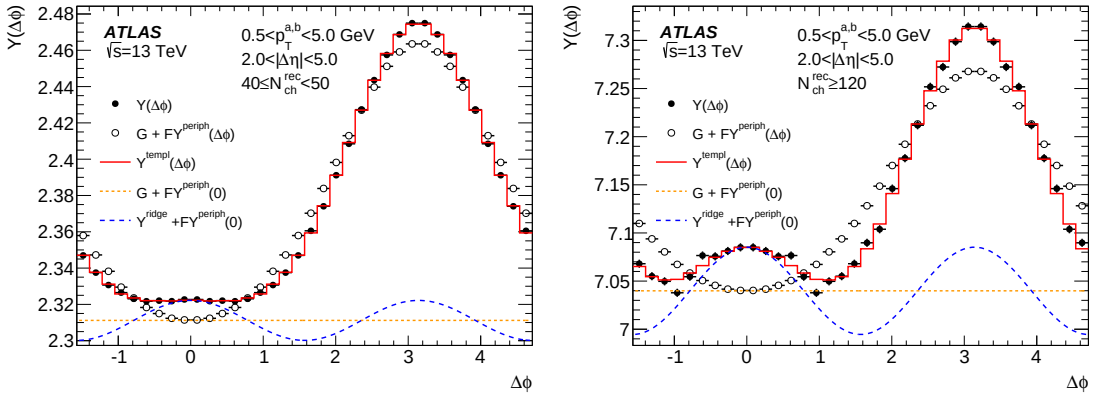

Figure 3: Per-trigger-particle yields, $Y(\Delta\phi)$, for $0.5 < p_{\text{T}}^{\text{a,b}} < 5.0$ GeV in different $N_{\text{ch}}^{\text{rec}}$ intervals in 13 TeV pp data. Results are shown for $40 \leq N_{\text{ch}}^{\text{rec}} < 60$ (left panel) and for $N_{\text{ch}}^{\text{rec}} \geq 120$ (right panel). The open points and curves show components of the template [11].

modulations arise from a modulation of the single-particle ϕ distributions, then $v_{\text{n,n}}(p_{\text{T}}^{\text{a}}, p_{\text{T}}^{\text{b}})$ should factorise into a product of single particle harmonics $v_{\text{n}}(p_{\text{T}}^{\text{a}})v_{\text{n}}(\text{p}_{\text{T}}^{\text{b}})$. Detailed study showed [11, 12] that the factorisation holds for $v_{2,2}$, $v_{3,3}$ and $v_{4,4}$ up to $p_{\text{T}} \approx 5$ GeV, and within this p_{T}-range the single particle harmonics can be calculated as $v_{\text{n}} = \sqrt{v_{\text{n,n}}}$.

3. Results

Figure 4 shows the second order Fourier harmonics v_2 obtained with the template fitting method for pp collisions at energy of $\sqrt{s} = 2.76$ and 13 TeV as a function of the charged particle multiplicity $N_{\mathrm{ch}}^{\mathrm{rec}}$. The measurement shows that v_2 weakly depends on multiplicity and is consistent across the two energies of pp collisions. This first measurement of v_2, shown in

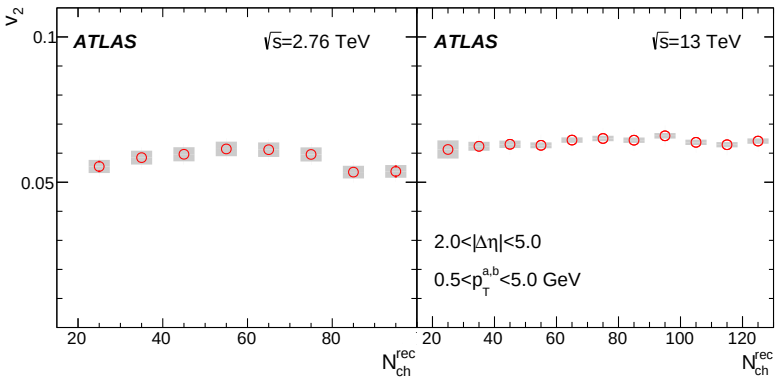

Figure 4: The measured v_2 as a function of $N_{\mathrm{ch}}^{\mathrm{rec}}$ for $0.5 < p_{\mathrm{T}}^{\mathrm{a,b}} < 5.0$ GeV in 2.76 TeV (left) and 13 TeV (right) pp data [11].

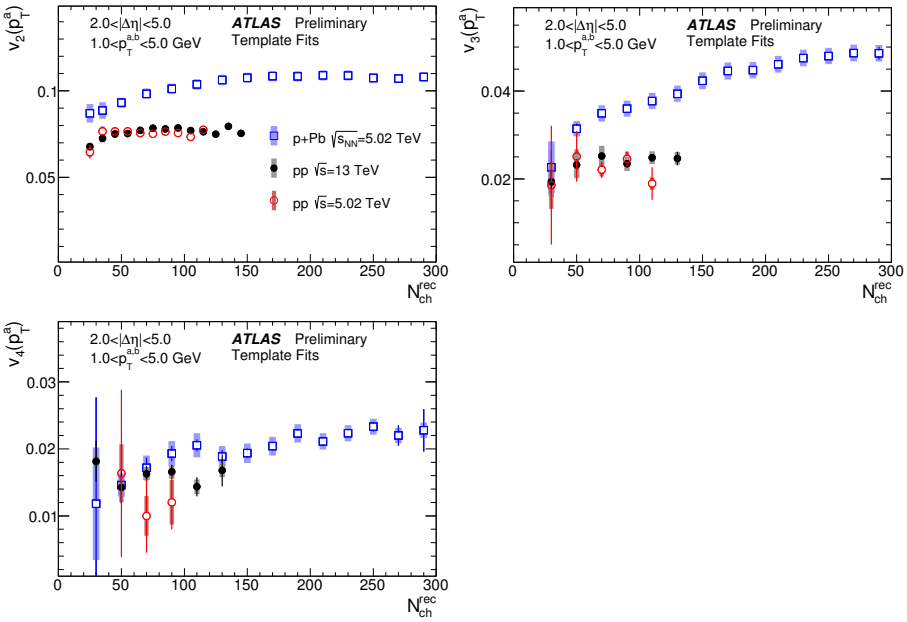

Figure 5: Comparison of the v_{n} obtained for the 13 TeV pp, 5.02 TeV pp, and 5.02 TeV p+Pb data, as a function of $N_{\mathrm{ch}}^{\mathrm{rec}}$. The results are for $1 < p_{\mathrm{T}}^{\mathrm{a,b}} < 5$ GeV. The three panels correspond to n=2, 3 and 4 [12].

Fig. 4, was recently complemented with additional measurements of v_2, v_3 and v_4 harmonics in 5.02 TeV pp, 13 TeV pp, and 5.02 TeV p+Pb data, shown in Fig. 5 as a function of $N_{\mathrm{ch}}^{\mathrm{rec}}$, for the $1 < p_{\mathrm{T}}^{\mathrm{a,b}} < 5$ GeV interval. The figure shows that all three v_{n} harmonics in the 5.02 and 13 TeV pp data are $N_{\mathrm{ch}}^{\mathrm{rec}}$-independent, while the p+Pb v_2, v_3 and v_4 increase with increasing $N_{\mathrm{ch}}^{\mathrm{rec}}$. Generally,

all three harmonics in pp collisions are smaller than corresponding v_n harmonics in p+Pb collisions.

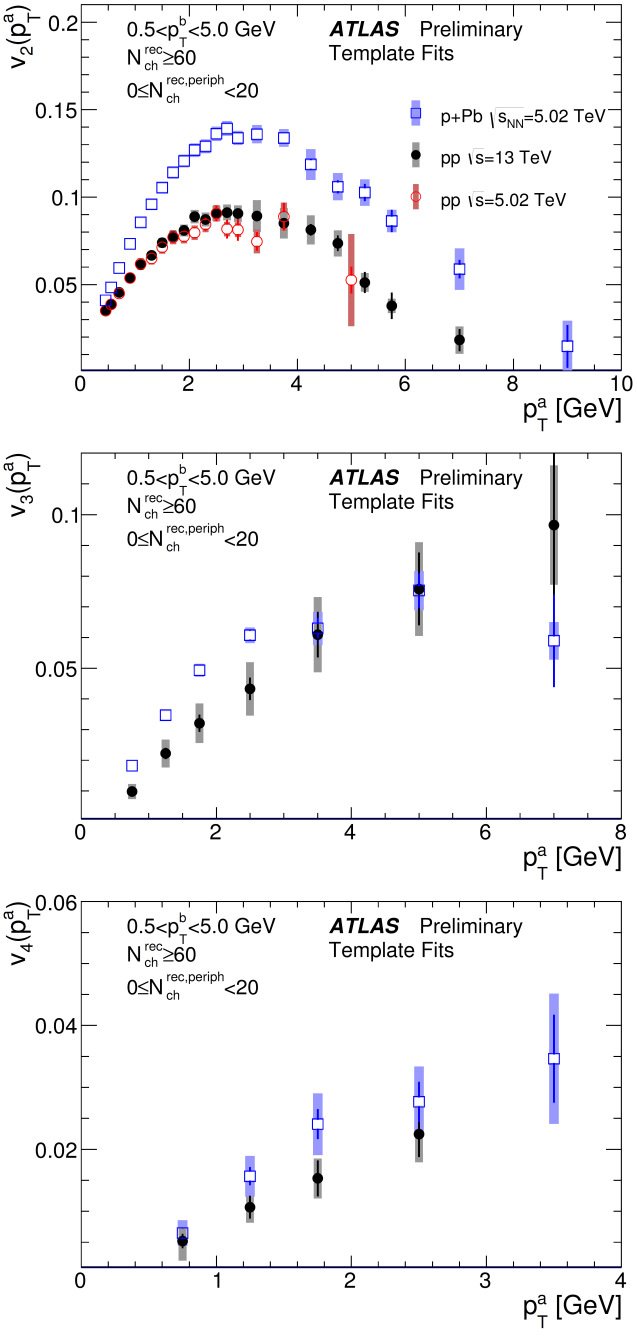

Figure 6: The p_{T} dependence of the v_n in 13 TeV pp, 5.02 TeV pp, and 5.02 TeV p+Pb collisions for the $N_{\mathrm{ch}}^{\mathrm{rec}} \geq 60$. Panels from top to bottom correspond to n=2, 3 and 4 respectively [12].

Figure 6 shows, the transverse momentum dependence of $v_{\mathrm{n,n}}$ harmonics in 13 TeV pp, 5.02 TeV pp, and 5.02 TeV p+Pb collisions for $N_{\mathrm{ch}}^{\mathrm{rec}} \geq 60$. The v_2 values in pp collisions at both energies are similar. As a function of transverse momentum, at first, they rise reaching a maximum near 3 GeV and for higher p_{T} they drop, reaching almost 0 at $p_T \approx 7$ GeV. In p+Pb collisions a more rapid increase of elliptic flow is measured but generally a similar trend of the p_{T} dependence is observed in both systems. The triangular harmonic in 13 TeV pp increases with p_{T} over the whole measured p_{T} range. For p+Pb collisions, within p_{T} range up to 3 GeV, larger v_3 values are observed than in pp. At higher p_{T}, v_3 in p+Pb data saturates. The v_4 values in 13 TeV pp and 5.02 TeV p+Pb collisions increase within the measured p_{T} range and larger v_4 harmonic is found in p+Pb collisions as compared to pp data.

The previous ATLAS measurements [14, 15] have shown that in Pb+Pb collisions v_4 and v_2 harmonics are non-linearly correlated. This correlation may result from a response of the medium to the initial elliptic eccentricity, which can contribute to quadrangular azimuthal modulations in the particle production. In Pb+Pb collisions, the non-linear contribution to v_4 is found to dominate over the geometric contribution, except of the most central collisions where the initial-state fluctuations are large and prevailing. It is expected that in the scenario of a large non-linear contribution to v_4, proportional to v_2^2,

the ratio v_4/v_2^2 should to be constant. Figure 7 shows v_4/v_2^2 as a function of $N_{\rm ch}^{\rm rec}$ for 13 TeV pp and 5.02 TeV p+Pb collisions. The ratio is indeed observed to be approximately constant as a function of $N_{\rm ch}^{\rm rec}$ and is found to be about 50% larger in pp than in p+Pb collisions.

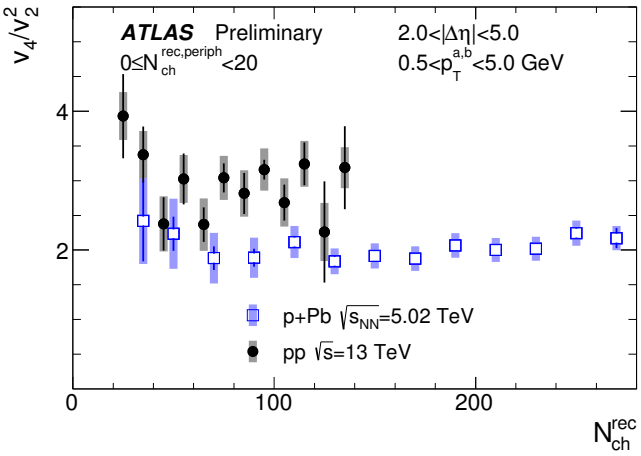

Figure 7: Ratio of the $v_{\rm n}$ to the v_2^2 as a function of $N_{\rm ch}^{\rm rec}$ in the 13 TeV pp and 5.02 TeV p+Pb data. The results are for $0.5 < p_{\rm T}^{\rm a,b} < 5$ GeV [12].

4. Summary

A template fitting procedure was used to obtain single-particle $v_{\rm n}$ harmonics (n=2, 3, 4) in pp collisions at $\sqrt{s}$ = 2.76, 5.02 and 13 TeV and in p+Pb collisions at $\sqrt{s_{\rm NN}}$= 5.02 TeV as a function of multiplicity and transverse momentum. The measurement shows that v_2 in pp collisions weakly depends on multiplicity and is consistent between the three collision energies. The p+Pb v_2 values are larger than the pp v_2 for all multiplicities and are observed to increase with $N_{\rm ch}^{\rm rec}$. As a function of $p_{\rm T}$, p+Pb v_2 is larger than v_2 in pp collisions but similar $p_{\rm T}$ dependence is observed, which also resembles the trend seen in Pb+Pb collisions, i.e. at low $p_{\rm T}$ v_2 rises reaching a maximum near $p_{\rm T}$ = 3 GeV and for higher $p_{\rm T}$ v_2 drops. Similarly to the results for v_2, the pp v_3 and v_4 values are consistent with being independent of $N_{\rm ch}^{\rm rec}$ within uncertainties, while the p+Pb values are observed to increase with $N_{\rm ch}^{\rm rec}$. The v_4/v_2^2 ratio is found to be $N_{\rm ch}^{\rm rec}$-independent for both the 13 TeV pp and the p+Pb data. This ratio is observed to be about 50% larger in pp than in p+Pb collisions.

This work was supported in part by the National Science Centre, Poland grant 2015/18/M/ST2/00087 and by PL-Grid Infrastructure.

References

[1] S. A. Voloshin, A. M. Poskanzer, and R. Snellings, Elementary Particles, Nuclei and Atoms (Springer-Verlag) **23** (2010) 293, arXiv:0809.2949 [nucl-ex].

[2] ATLAS Collaboration, Phys. Lett. B **707** (2012) 330, arXiv:1108.6018 [hep-ex].

[3] ATLAS Collaboration, JHEP **11** (2013) 183, arXiv:1305.2942 [hep-ex].

[4] ATLAS Collaboration, EPJ C **74** (2014) 2982, arXiv:1405.3936 [hep-ex].

[5] ATLAS Collaboration, EPJ C **74** (2014) 3157, arXiv:1408.4342 [hep-ex].

[6] ATLAS Collaboration, Phys. Lett. B **725** (2013) 60, arXiv:1303.2084 [hep-ex].

[7] ATLAS Collaboration, Phys. Rev. C **86** (2012) 014907, arXiv:1203.3087 [hep-ex].

[8] ATLAS Collaboration, Phys. Rev. C **90** (2014) 044906, arXiv:1409.1792 [nucl-ex].

[9] ATLAS Collaboration, Phys. Rev. Lett. **110** (2013) 182302, arXiv:1212.5198 [hep-ex].

[10] CMS Collaboration, JEP **09** (2010) 091, arXiv:1009.4122 [hep-ex].

[11] ATLAS Collaboration, Phys. Rev. Lett. **116** (2016) 172301, arXiv:1509.04776 [hep-ex].

[12] ATLAS Collaboration, ATLAS-CONF-2016-026 (2016). http://cds.cern.ch/record/2157690.

[13] ATLAS Collaboration, JINST **3** (2008) S08003.

[14] ATLAS Collaboration, Phys. Rev. C **90** (2014) 024905, arXiv:1403.0489 [hep-ex].

[15] ATLAS Collaboration, Phys. Rev. C **92** (2015) 034903, arXiv:1504.01289 [hep-ex].